

Fabrication of 3D micro and nanostructures for MEMS and MOEMS: an approach based on combined lithographies.

This article has been downloaded from IOPscience. Please scroll down to see the full text article.

2006 J. Phys.: Conf. Ser. 34 904

(<http://iopscience.iop.org/1742-6596/34/1/150>)

View [the table of contents for this issue](#), or go to the [journal homepage](#) for more

Download details:

IP Address: 155.69.4.4

The article was downloaded on 15/11/2012 at 15:06

Please note that [terms and conditions apply](#).

Fabrication of 3D micro and nanostructures for MEMS and MOEMS: an approach based on combined lithographies.

F. Romanato^{1,2}, **L. Businaro**¹, **M. Tormen**¹, **F. Perennes**³, **M. Matteucci**³, **B. Marmioli**³, **S. Balslev**⁴ and **E. Di Fabrizio**^{1,5}

1 Lab. TASC-INFN-CNR at Elettra synchrotron, S.S. 14 km 163.5, 34012 Trieste (Italy)

2 Nanyang Technological University, SME, 50 Nanyang Ave. Singapore 639798

3 Sincrotrone Trieste, Area Science Park, I-34012 Basovizza-Trieste, Italy

4 MIC- Department of Micro and Nanotechnology, Technical University of Denmark (DTU), DK-2800 Kongens Lyngby, Denmark

5 BIONEM Lab, Universita' Magna Graecia, Campus Germaneto, viale Europa 88100, Catanzaro, Italy

Abstract. X-ray lithography is an established technique for the micro fabrication of MEMS and MOEMS well known for low sidewall surface roughness, submicron critical dimension, and high aspect ratio. Recently the typical characteristics of this technique has been developed approaching new opportunities deriving by the possibility to perform tilted exposure and by the combined use with electron beam lithography that allow to shape with direct patterning already the final material in 3D micro and nanostructures. The general approach is to concentrate the complexity of the multi layer fabrication process required to obtain 3D nanostructures mostly on the lithographic process. This capability represent a micro- and nanofabrication tool enabling new technologies. In this paper will be shown a multiple-tilted X-ray lithography procedure combined with e-beam lithography to create sub-micrometric patterns of arbitrary shape buried in 3D structure. The use of deep x-ray lithography in multi exposure configuration has been also exploited for the production of biodegradable 3D scaffold structures and of micro needles based transdermal delivery tools fabrication.

1. Introduction

New methods for micro- and nanofabrication are becoming essential to scientific progress in many disciplines. They form enabling technologies for applications ranging from plastic electronics to nano-electromechanical systems, from micro-optical components to microfluidic devices for molecular diagnostics or bio-medical purposes. In many cases, advances are aided by the highly engineered lithographic technologies developed for microelectronics. However, the layer-by-layer approach of industrial microelectronic fabrication methods required by high throughput and standardization level provides some obvious limitations in terms of resolution, ability to reproduce features with complex and three dimensional (3D) shapes, topography and material and chemical incompatibility with many organic and biological materials. New trends in fabrication methodology look forward to lithography techniques with intrinsic 3D structuring capabilities. The general idea is to push the complexity of the fabrication on the lithographic process in order to minimize and simplify the subsequent processing steps.

Several lithographic techniques have intrinsic 3D structuring capabilities. For example, Electron beam lithography (EBL) can generate “*gray-scale*” profiles by controlling the exposure dose. X-ray lithography (XRL) is capable to replicate multilevel masks by amplifying the thickness profile¹ and could generate

complex 3D structures with multiple exposures at tilted angles^{2,3}. Also, focused ion beam (FIB) lithography has shown capability for direct milling and growth of hard materials⁴. Nano-imprint lithography can mould 3D profiles⁵. Two photon polymerized lithography can directly sculpture microstructure⁶. Holographic lithography can generate large volume periodic 3D structure at sub micrometer resolution⁷. All these lithographic techniques have their own peculiarities and potentialities that in many cases cannot be exploited to completely cover the entire spectrum of fabrication needs. Many of this limitation can, on the contrary, be overcome combining the peculiarities of different lithographies in hybrid lithography approach. In this perspective the present overview focus on current research at LILIT lab (Laboratory for Interdisciplinary Lithography) - on combined lithographies and tilted multi-exposures X-ray lithography approach .

2. Multiple-exposures x-ray lithography for 3-D patterning

In XRL, conventionally, the mask+wafer assembly is held perpendicularly to the beam. During the one-to-one mask pattern projection on the resist a vertical, digital-like, lithographic profile is provided. However, the idea underlying the realization of 3D pattern structuring by *multiple-tilted x-ray lithography* is based on unconventional exposure geometry. The schematics of this geometry is shown in fig .1.

The mask + wafer are mounted at a tilted angle with respect to the x-ray beam so that, seen from the surface of the wafer, each opening of the x-ray mask behaves as a collimated light source exposing the resist along a tilted direction (fig. 1.a). A 180° azimuth angular rotation around the axis perpendicular to the mask-sample system will generate a second exposure along a different direction (fig. 1.b). The relative position of mask+wafer is kept fixed during the rotation and, due to the fact that no further alignment is required, the multiple-tilted-exposure at different angles can be regarded simply as an independent single step process. The concept of multiple-tilted x-ray lithography has been implemented in fabrication of 3D structure^{8, 9} originally conceived for the fabrication of photonic crystals with yablonovite structure. The infiltration with noble metals made these 3D lattice very interesting for photonic crystals in the terahertz frequencies range. In fig 2.a it is shown a metallic photonic crystal working at 100THz. This fabrication approach has been used to fabricate *metallic filter sieves* exploiting specifically designed X-ray masks. An example of such vertical gratings with well defined porosity is illustrated in fig. 2.b and 2.c. obtained by the intersection of high aspect ratio inclined pillars. These metallic sieves could offer advantage in using them as cathodes in microfluidic devices for sorting different ionic species.

The basic technology used is the 3D *deep x-ray lithography* (DXRL) technique is often used to produce casting moulds offering both sufficient resolution and mechanical stability with reasonable outer dimensions within reasonable time. With DXRL polymer structures of aspect ratio up to 100:1 can easily be obtained. We are also exploring its use in multi exposure configuration for the production of biodegradable 3D scaffold structures and devices to enable the in-vitro assembly of complex 3D cell structures for tissue replacement and regeneration. These novel systems should allow the perfusion of the growing tissue reducing nutrient limitations.

The considered *scaffold geometry* consists in a 5 mm side cube with interconnected circular pores of 50 µm diameters each separated by 180 µm. The first DXRL exposure was performed on a 5 mm thick PMMA sheet to cut off the 5 mm side cube as well as partially etch the first array of pores (Fig. 3). The second and third exposures were then performed changing the orientation of the cube versus the beam direction as shown in (Fig. 3). The 3D interconnection of the pores requires a perfect alignment of the mask with pre-etched pores for the second and third exposition. After the third exposure the cube was immersed in the developing solution for a total developing time of 60 hours. A SEM micrograph showing fabricated 3D scaffold in PMMA after the three DXRL exposures is shown in fig. 4. A magnified view of the cube corner shows the three perpendicular axes in etched struts.

The main issue of concern was the ability to develop the 100:1 aspect ratio pores over the entire length of 5 mm. The dynamic of the removed PMMA particles is slowed because they tend to be trapped inside the deep channels and block the further access of the developing solution to the remaining exposed PMMA. Megasonic supported development enhances the current of the developer inside the pores¹⁰ and increase the developing rates by 4 times¹¹.

The definition of the most adequate *scaffold* design and the correspondent required properties is mainly determined by the tissue engineering approach selected for the regeneration of a specific tissue, as the scaffold must be able to induce the desired tissue response. 3D porous structures have been recognized as the most appropriate design to sustain cell adhesion and proliferation. For these reasons, it is considered essential to have a method of creating *biomaterial scaffolds* having a known and well-defined topology. Several methods for the deposition of biopolymers with controlled or *scaffolds* architecture have been described in

the literature^{12,13,14}. We want underline that this proposed technique (DXRL) in multi exposure configuration for the production of *biodegradable 3D scaffold structures* and devices allows a precise design of the structure and porous dimension that can be applied to specific geometrical topology.

The fabrication of bevelled microneedles in hard polymer accomplished by use of different processes like hot embossing, DXRL, and casting. A PMMA sheet with a periodic 3D groove profile corresponding to the pitch size of the needle array was fabricated by hot embossing using a mould fabricated by conventional micromachining techniques. The embossed PMMA sheet was then glued on a substrate coated with a base plating layer. The X-ray exposure projects the triangular cross-section on the inclined wall of the PMMA grooves and after development the array of sharp-bevelled microneedles is formed. The bevel angle is determined by the angle of the groove inclined wall versus the horizontal plane. A Nickel layer is electroplated with a thickness corresponding to the height of the base of the future micro-needle array. A second DXRL exposure is performed masking only the needle array to irradiate the PMMA alignment marks. During a second developing step the remaining PMMA inside the channels and the alignment marks are removed. An example of bevelled microneedles with a triangular cross-section is shown in fig. 5.

It was recently shown that a soft material like Polyvinil Alcohol (PVA) can advantageously replace the more common PDMS because it is soluble in water¹⁵. The PVA inverse mould is then use to cast the final microneedle array with a liquid polymer solution that solidifies in a few hours at room temperature (i.e. PMMA). Then the PVA mould is simply dissolved in water releasing the final microneedle array in PMMA.

3. Binary resist process for hybrid lithography

An hybrid lithography based on *binary resist process*¹⁶ and combining two different lithographies, EBL and XRL, has been developed for the fabrication of suspended structures and for the realization of arbitrary shaped patterns embedded inside three dimensional structures. The layout of the process is shown in fig. 6.

The developed process utilizes the combination of a low sensitivity positive tone resist, PMMA, and a high sensitivity negative resists, SAL-607 ER7¹⁷. A 5 μm layer of PMMA has been previously spun and baked at 170 degv (Fig. 6.a). Then a film of SAL-607 ER7 is spun on top of PMMA layer (Fig. 6.b). The double layer have been baked on at 105°C for 1min. Several parallel lines of different thickness have been patterned by EBL on a 300nm thick SAL-607 ER7 film. The wire widths were decreased from 800nm to 200nm in step of 200nm. The exposure dose was 10 $\mu\text{C}/\text{cm}^2$ (Fig. 6.c). The low threshold dose of SAL-607 ER7 allows performing the electron beam lithography almost completely unaffected the bottom layer PMMA resist owing to its low sensitivity. The process on the negative resist, completed with post baking and development, results in a chemically stabilized polymeric pattern of the designated pattern lying on the top of the first (bottom) PMMA layer are resulted (Fig. 6.d). Subsequently, a second PMMA coating is spun and normally baked (Fig. 6.e). At this juncture, XRL was performed either in the usual vertical configuration (Fig. 6.f) or in the *multiple-tilted configuration*. The SAL-607 ER7 structure at this point is completely embedded in the PMMA resist structure which can be used as template for a final electroplating metal growth (Fig. 6.g). The fundamental characteristic that allows performing the X-ray lithography on the whole resist structure is that SAL-607 is *transparent* to X-ray but remains *mechanically* and *chemically stable*. The successive developing of the structure in the PMMA does not invalidate the defect patterning at the interface.

The *binary resist process* has successfully been applied for the fabrication of several 3D test structure: a suspended wires formed in SAL-607 ER7 (by EBL) bridging the PMMA rectangular pillar and cylinders fabricated by XRL (fig. 7.a -c). Some of the wires collapsed exclusively due to a lack of suspension support at one of the edges resulted because of misalignment with vertical pillars. However, in the case of bi-directional suspension, no sagging was observed along the 20 μm air-born-step, even for the thinnest wires of 200nm. On the contrary, for 50 μm bridged air-steps, only wires of 200 nm or smaller size collapsed (Fig. 7.b-c). In principle, by using a layer-by-layer approach, few nano-meters of tolerance are admissible in-order to avoid pillar SAL-601 misalignments. This accuracy will certainly require a comprehensive alignment technique not available at present on our sample holder. This problem is, however, completely overcome by performing a *unique* XRL exposure that determines a self alignment of the structures. As a matter of fact, no evidence of discontinuities along the PMMA pillars were noticed (Fig. 7.c).

This structure represents a symbolic test pattern that, however, can be used as template to be converted into a *flyover channels*. This structure represents one of the basic building blocks for the realization of micro-fluidic networking, by which different liquids can be flushed independently along intersecting trajectories without mixing¹⁸. The importance of this element increases together with the complexity and the number of liquids to be processed on the chip that generally requires a strategic organization of the channel network where also the vertical dimension plays a critical role.

To obtain the flyover channel it is necessary to invert the tone of the template structure in order to transform the pillars into fluid reservoirs and wires into tubes connecting reservoirs. This can be easily obtained with metallic electrolytic growth by exploiting the metallic film base plating (as cathode) on which the resist template has been realized. The gold electrolytic growth progressively overwhelms the resist wires that finally result embedded in a gold structure grown up to the top of the cylindrical PMMA micro reservoirs. Removal of residual PMMA performed with hot acetone. A top view of the fabricated structure is shown in (Fig. 7.d) where one can see the presence of left-over embedded SAL-601 wires that we have deliberately left for sake of clarity.

New fabrication perspective come from the combination of above described binary resist technique and the direct patterning of final materials. The idea of the direct patterning is that the resist should not be considered as a sacrificial layer of a process, but already the final material for the sample. In addition, it is possible to functionalize the transparent resist by doping it with organic fluorescent dyes, thereby enabling devices made in the resist to act as fluorescent emitters of light, light amplifiers and lasers¹⁹. The first example in this case is given by Kristensen et al.²⁰ who showed that the well known SU8 resist doped with Rhodamine is sufficiently hard polymeric material with appropriate index of refraction that can be used for final material in several photonic application^{21, 22}. To show this potentiality in combination with the binary resist process we have fabricated a suspended waveguide selectively doped with organic dye. The dye doped SU-8 was prepared by mixing Rhodamine 6G powder in SU-8 thinner (GBL) and subsequently mixing the doped thinner in SU-8 10. The doped SU-8 was subsequently spun on PMMA yielding a second layer with a thickness of around 3 μm . This system was baked for 2 min at 90 °C prior to exposure and post baked at 90 °C for 20 min before development in PGMEA for 30 s and rinsed in isopropyl alcohol. Electron beam lithography was performed at 30 keV exposing the SU8 top layer with a dose of 3 $\mu\text{C}/\text{cm}^2$. Then the SU8 was post baked for 20 min at 90°C and then developed in PMGEA for 30 sec and rinsed in IPA in order to achieve the waveguide profile. Subsequently the whole structure was exposed with X-ray in order to generate the trenches in PMMA. The exposure dose was 6 J/cm^2 and the development in MIBK1:1IPA was 70sec long. Fig. 8 shows a SEM micrograph of a SU8 waveguide suspended on a patterned PMMA substrate. This structure was obtained following the two binary process previously described. The same structure was also observed in fluorescence mode with an optical microscope to show the fluorescence only of the suspended waveguide. This preliminary structures shows the possibility not only to dope SU8 in order to use an optical active material but also the possibility to selectively dope SU8 when used in combination with other resists in order to obtain 3D patterning.

However to fully show the capability of doped SU8 as optical material in combination with x-ray lithography, we have used it to demonstrate light sources²³. The structure is an amplified spontaneous emission (ASE) light source that couples out light normal to the chip plane. The dye embedded in the SU-8 is optically excited by an external light source tuned to the absorption band of the dye. The waveguiding action is obtained by refractive index confinement. SU8 that has refractive index $n=1.6$ is deposited on a silicon dioxide substrate surface and surrounded by air. The waveguide structure terminates with flat inclined end-surface walls fabricated by tilting the x-ray mask and substrate assembly 45° relative to the x-ray beam during lithography see Fig. 9. The tilted end acts as a mirror that reflects light traveling in the waveguide upwards and away from the chip surface by total internal reflection. Thereby one end surface of the waveguide will be shaped in a triangular fashion that couples out light in the vertical direction compared to the chip plane. When the laser dye in the waveguide is excited optically from the outside, the fluorescence is guided to the ends of the waveguide. If the optical pumping of the dye has inverted the population of the electronic states of the dye, the spontaneous emission will be amplified as it travels down the waveguide (ASE) and the light output will increase dramatically as compared to pure fluorescence.

4. Conclusions

We have reviewed our research activities of X-ray lithography in combination with electron beam lithography for the fabrication of various functioning 3D micro and nano structures and devices and MEMS structures for existing and potential emerging diverse applications mainly oriented in our purpose to bio sensor and medical application. The structures generated shows either high resolution, high aspect ratio and moreover allow to design complex 3D structures otherwise impossible. We have also shown that this techniques can further extended with the application of a two resist process that can be used in combination with electron beam lithography. The results shows the possibility to generate self standing structure suspended above the substrate surface. Finally this process have applied to doped SU8 photonic structure

that have shown to be selectively doped on surrounding other resist and therefore opening the possibility to a 3D photonic networking in MOEMS systems.

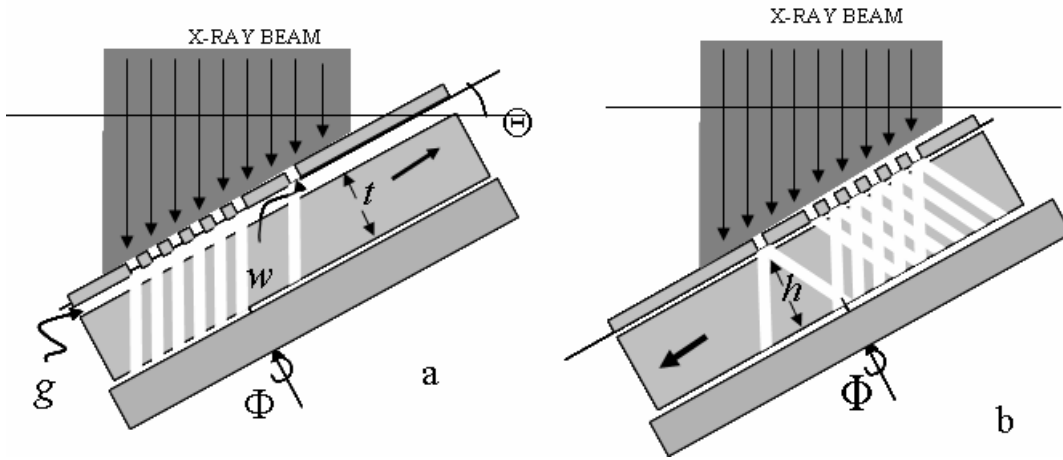


Fig.1 (a) Scheme of a tilted exposure. The X-ray mask is large as the beam width. The tilt angle θ , the azimuth angle ϕ , the pattern width w , the mask-sample gap g and the resist thickness t are shown. (b) Scheme of the exposure geometry after 180° azimuth rotation. The height, h , of the channel is shown.

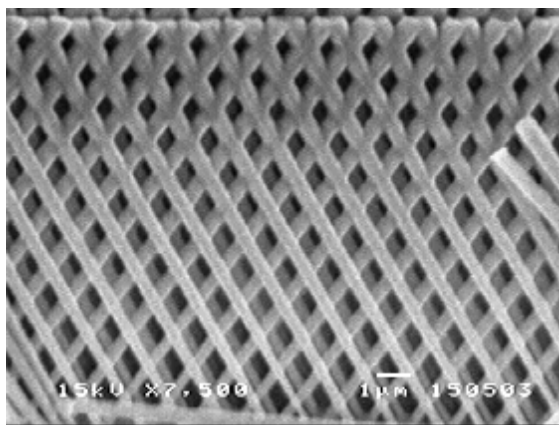


Fig. 2.a

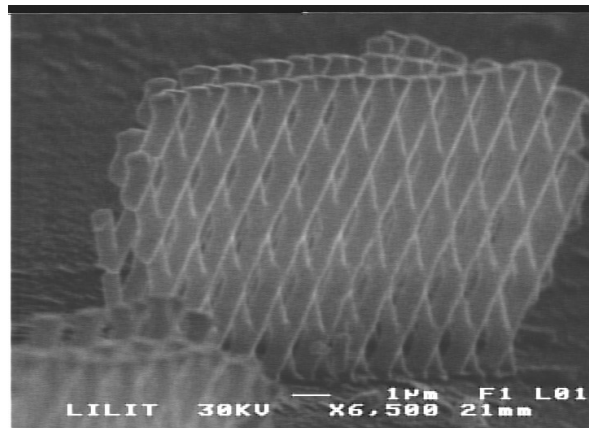


Fig. 2.b

Fig 2. (a) Electrolytically grown Au yablonovite structure obtained by three tilted X-ray exposures of the same mask along different directions. (b) Intersected high aspect ratio pillars array can also be sequenced in several vertical layers of filters for their possible application as electrode in electrochemical micro sensors.

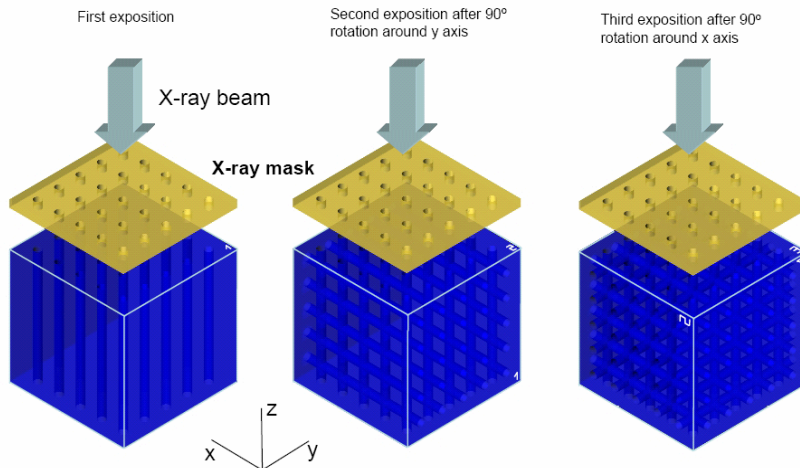


Fig. 3 DXRL fabrication process of the 3D scaffold in PMMA.

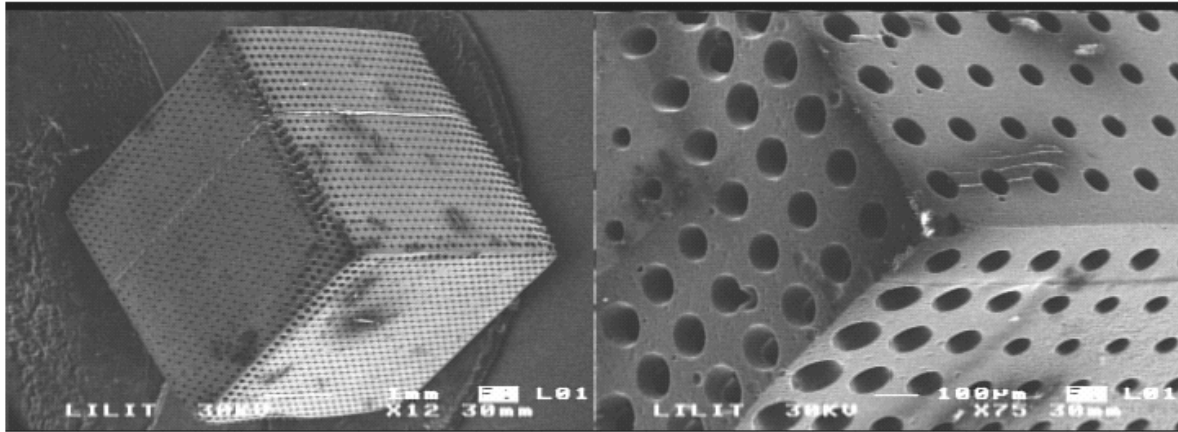


Fig. 4 PMMA 3D scaffold. The intersecting pillars array can also be sequenced in several vertical layers of filters for their possible application as electrode in electrochemical micro sensors.

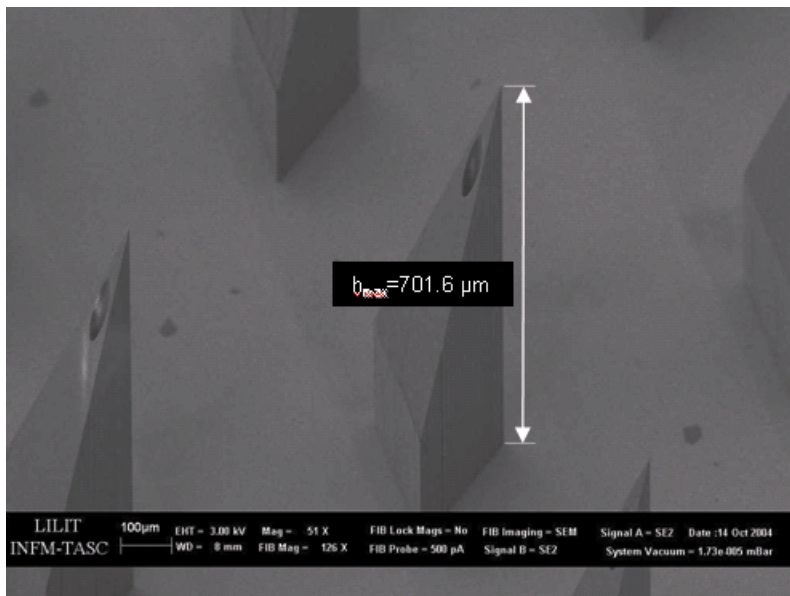


Fig. 5 PMMA microneedles obtained by deep X-ray lithography on embossed PMMA sheet,

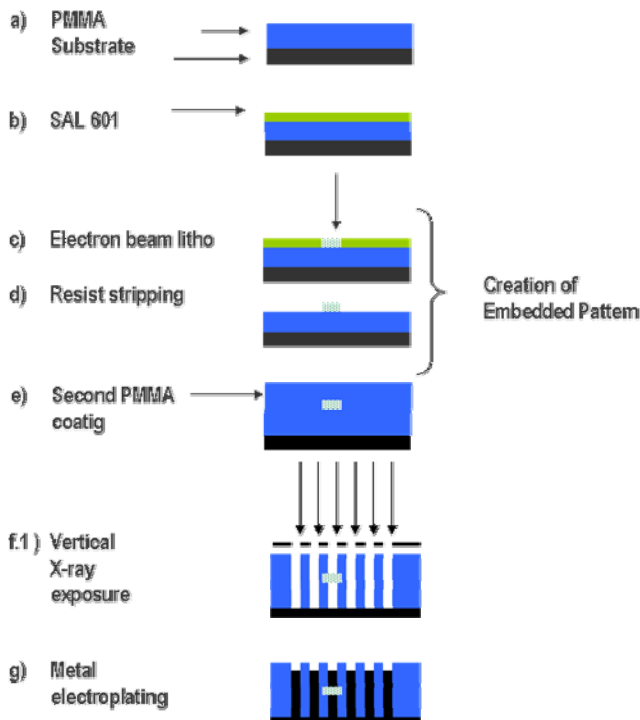


Fig. 6 Binary resist process flow scheme. Two resist are combined with two distinct lithography. After a first PMMA coating and baking (a), a second resist (SAL-607 ER7) is spun, baked (b), exposed by Electron beam lithography (c) and normally developed (d). In the following a second PMMA coating is spun and normally baked (e). At this point x-ray lithography can be performed either in the usual vertical configuration (f). The SAL-607 ER7 structure at this point remains unchanged resulting completely embedded in the in the PMMA resist structure that can be used as template for a final electroplating metal growth (g).

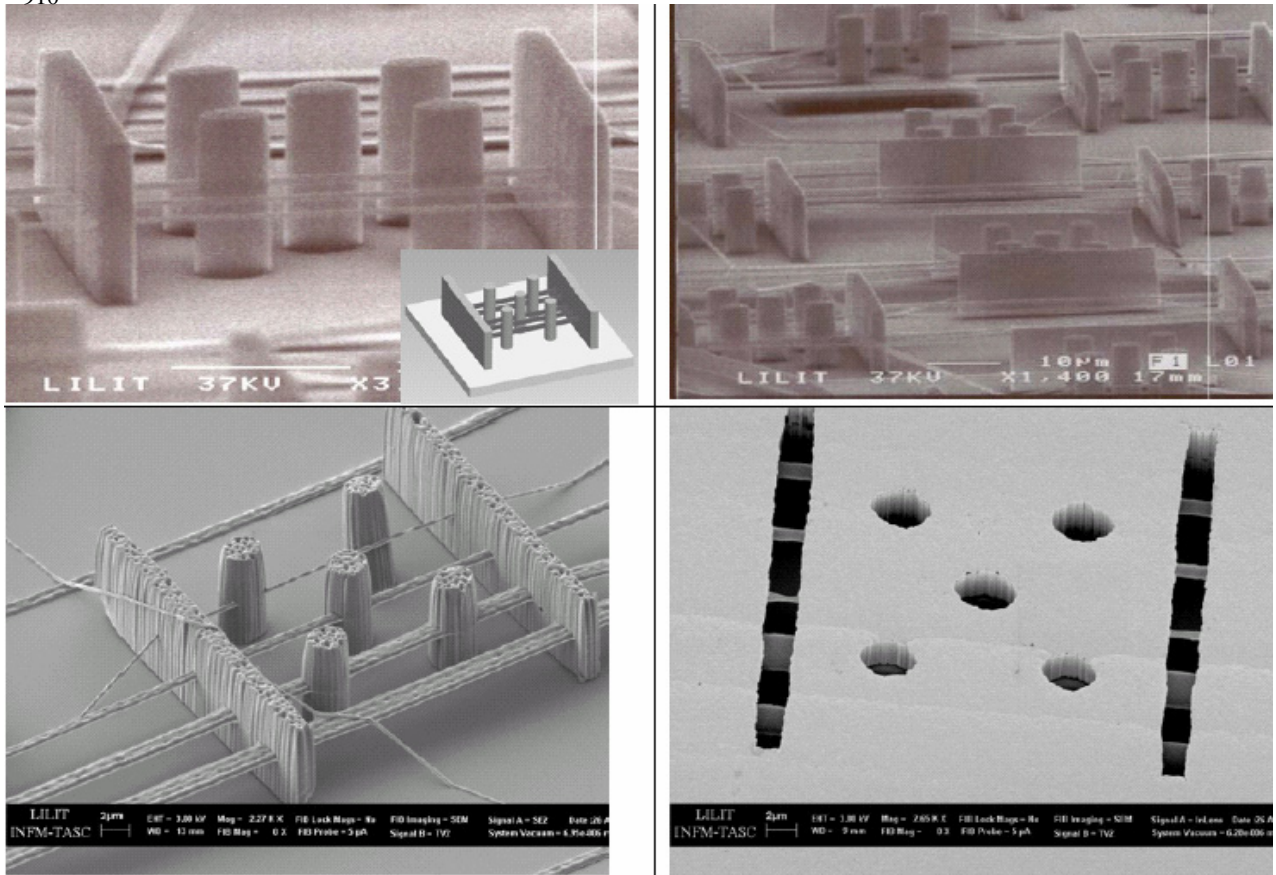


Fig. 7 . Wires made of SAL 601 resist suspended between vertical PMMA pillars representing micro tanks whose model is sketched in the inset. SEM micrographs showing in (a) & (b) the fabricated wire with different size made in SAL 601 resist, (c) illustrating linear defect (generated by electron beam lithography with different doses) parallel to the substrate and inserted at the interface of two 3-D lattices. (d) Top view of the microfluidic channels embedded in a gold matrix after the dissolution of the PMMA structure. The tubes are still filled by SAL resist for sake of clarity.

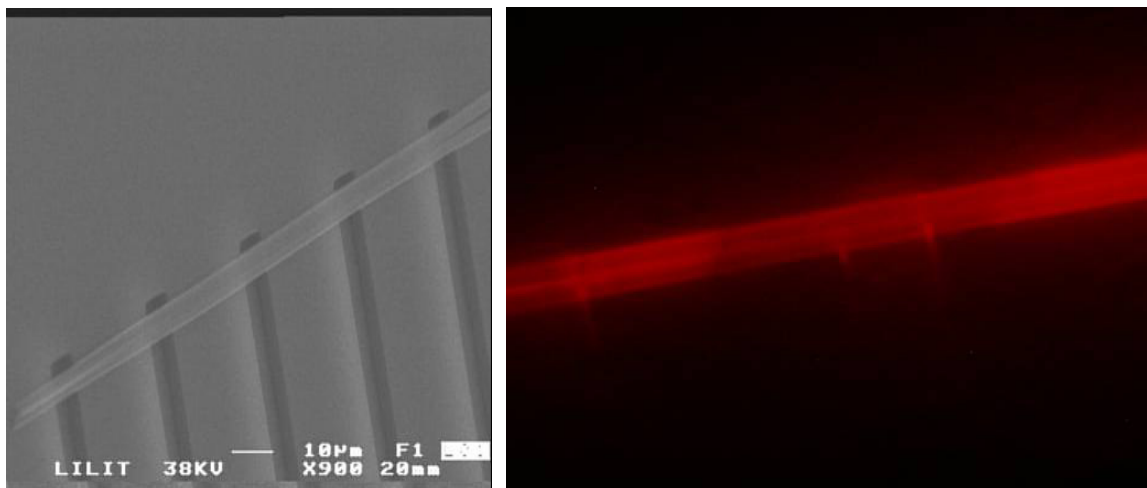


Fig. 8 Left: SU8 waveguide patterned on the top a PMMA patterned layer following the binary resist process for the realization of suspended structures. Right: Fluorescence from the same SU8 waveguide as in the left figure that has been selectively doped with Rhodamine.

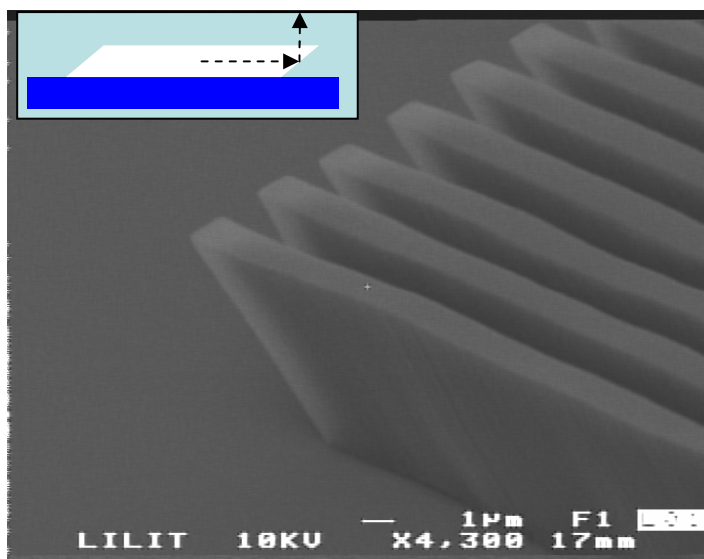


Fig. 9 Detail of the 45° tilt end edge of trapezoidal waveguide (see insert) obtained by tilted x-ray lithography and designed to obtain light from amplified stimulated emission from the Rhodamine 6G dye embedded in the waveguide polymer matrix.

¹ Cabrini S, Gentili M, Di Fabrizio E, Gerardino A, Nottola A, Leonard Q, Mastrogiacomo L;; MICROELECTRONIC ENGINEERING 53 (1-4): (2000) 599-602

² M. Han, W. Lee, S. K. Lee, S. S. Lee,; Sensors and Actuators A 111 (2004) 14–20;

³ F. Romanato, L. Businaro, L. Vaccari, S. Cabrini, P. Candeloro, M. De Vittorio, A. Passaseo, M.T. Todaro, R. Cingolani, E. Cattaruzza, M. Galli, C. Andreani, E. Di Fabrizio. Microelectronic Engineering 67-68 (2003), 679.

⁴ K.Wang, A. Chelnokov, S. Rowson, J. M. Lourtioz;; Appl. Phys. A 76, (2003) 1013–1016

⁵ Mingtao Li, Lei Chen, and Stephen Y. Chou; Appl. Phys. Lett., 78, 3322 (2001).

⁶ S. Maruo, O. Nakamura, S. Kawata; : Opt. Lett. 22 (2): (1997) 132-134

⁷ M.Campbell, D.N.Sharp, M.T.Harrison, R.G.Denning and A.J. Turberfield: Nature 404 (2000), 53.

⁸ Wolfgang Ehrfeld and Andreas Schmidt, Recent developments in deep x-ray lithography, J. Vac. Sci. Technol. B 16.6., Nov/Dec 1998

⁹ F. Romanato, L. Businaro, L. Vaccari, S. Cabrini, P. Candeloro, M. De Vittorio, A. Passaseo, M.T. Todaro, R. Cingolani, E. Cattaruzza, M. Galli, C. Andreani, E. Di Fabrizio: J. Vac. Sci. Technol. B. 51(2003), 2912.

¹⁰ P. Meyer, A. El-Kholi, J. Schulz, , Microelectronic Engineering, 63 (2002), 319.

¹¹ R.L. Bronaugh, H.I. Maibach, Percutaneous Absorption: Drugs-Cosmetics-Mechanisms-Methodology, Marcel Dekker, New York, 1999.

¹² Chu T. M. G., Orton D. G., Hollister S. J., Feinberg S. E. Halloran J. W.. Biomat., 23 (2002), 1283.

¹³ R. Landers, A. Pfister, U. Hübner, H. John, R. Schmelzeisen and R. Mülhaupt, J. of Materials Science, 37 (2002), 3107.

¹⁴ F. Pérennès, F. De Bona and F.J. Pantenburg, , Nucl. Inst. Meth. A, vol 467-468 (2001), 1274.

¹⁵ F. Perennes, B Marmioli, M Matteucci, M Tormen, L Vaccari and E Di Fabrizio, Sharp beveled tip hollow microneedle arrays fabricated by LIGA and 3D soft lithography with Poly vinyl alcohol, J. Micromech. Microeng. 16 (2006) 473-479.

¹⁶ Patent No. TO2003A000730 filed on 23.09.2003 F. Romanato, R. Kumar, E. Di Fabrizio.

¹⁷ SAL-607 ER7 is trademark of Shipley Inc.

¹⁸ Shize Qi, Xuezhu Liu, Sean Ford, James Barrows, Gloria Thomas, Kevin Kelly, Andrew McCandless, Kun Lian, Jost Goettert and Steven A. Soper, Lab Chip, 2 (2002), 88.

¹⁹ S. Kragh, S. Balslev, and A. Kristensen, Proceedings of the 7th International Conference on Miniaturized Chemical and Biochemical Analysis Systems _microTAS 2003_, Squaw Valley, CA, October 5–9, 2003, pp. 1331–1334.

²⁰ S. Kragh, S. Balslev, and A. Kristensen, Proceedings of the Seventh International Conference on Miniaturized Chemical and Biochemical Analysis Systems (microTAS 2003), Squaw Valley, California, USA, October 5-9, pp. 1331-1334, 2003

²¹ Z. Wang, J. El-Ali, M. Englund, T. Gotsaed, I. R. Perch-Nielsen, K. B. Mogensen, D. Snakenborg, J. P. Kutter, and A. Wolff, Lab Chip 4, 372 (2004).

²² Nilsson D, Nielsen T, Kristensen A,; REVIEW OF SCIENTIFIC INSTRUMENTS 75 (11): 4481-4486 NOV 2004

²³ Balslev S, Romanato F, Functionalized; JOURNAL OF VACUUM SCIENCE & TECHNOLOGY B 23 (6): 2910-2913 NOV-DEC 2005